NJC



PAPER



Cite this: New J. Chem., 2023. 47. 21190

implications for catalysts on oxide surfaces† John C. Hoefler, Da Yuan Yang* and Janet Blümel **

Adsorption of solid phosphines on silica and

Tertiary phosphines are ubiquitous in inorganic chemistry. They play important roles as ligands in coordination chemistry and catalysis. Furthermore, they act as surface acidity probes for oxide surfaces. However, only volatile phosphines, such as PH₃ have been applied in this function so far. Here we demonstrate for the first time that the triaryl- and trialkylphosphines PPh3 and PCy3 with high melting points self-adsorb readily onto a silica surface even in the absence of a solvent. The self-adsorption takes place within days when both solid components are mixed and then left undisturbed. The phosphines form well-defined monolayers on the surface and the transition from monolayer to left-over polycrystalline phosphine is abrupt. Therefore, the maximal surface coverage with a monolayer can be easily determined. When the phosphines are adsorbed from solutions, the same maximal surface coverage is found. Solid-state NMR spectroscopy provides a unique analytical tool for studying the structure and dynamics of phosphines in different environments. ³¹P and ²H solid-state NMR measurements are successfully applied for characterizing the adsorption process and the mobilities of the adsorbed phosphines across the silica surface. Furthermore, using $(Ph_3P)_2Ni(CO)_2$ as a representative, it is demonstrated that the silica surface has a hitherto unrecognized impact on immobilized and surface-residing catalysts because it competes for phosphine ligands coordinated to a metal center. This competition manifests as one more factor leading to the loss of phosphine ligands and ultimately leaching of immobilized metal complexes or nanoparticle formation. Besides the increase of fundamental knowledge about adsorption processes, the presented results have implications for chromatographic separations of metal complexes and for the lifetime of immobilized and other types of surface-residing catalysts.

Received 29th June 2023, Accepted 29th October 2023

DOI: 10.1039/d3nj03016d

rsc.li/njc

Introduction

The adsorption of molecules on a surface is ubiquitous in academia and industry and is applied for numerous analytical and purification purposes. In contrast to chemical bonding or immobilization, 2-4 the term physical adsorption is associated with a process where no electrons are transferred between the adsorbed molecules and the adsorbent surface. The interaction is caused mainly by van der Waals forces, and the adsorption is fully reversible. For example, volatile compounds are removed from a surface in vacuo. Alternatively, a nonvolatile adsorbate can be washed off with a favorable solvent.

Although adsorption is often disregarded when working with covalently bound species on a surface, it does have an impact on many systems and hitherto unrecognized implications. For example, immobilized catalysts²⁻⁵ are impacted by adsorption of ligands on support surfaces. The competition between the metal center and the surface for the coordinated phosphine can lead to a loss of the ligands and leaching of the metal from the surface as demonstrated in the Results and discussion section.

Neutral silica⁶ is the prevalent support for adsorption studies because of its mechanical stability during grinding, comparatively unreactive nature, and relatively large surface area of 750 m 2 g $^{-1}$. From a practical perspective, it easily packs into a solid-state NMR rotor and due to its large average particle diameters (0.062-0.2 mm) it can be handled in a glove-box or at the Schlenk line under an inert gas stream without dust issues. The adsorption results obtained with a silica surface for metallocenes^{7–10} and phosphine oxides^{11,12} translate to other surfaces such as alumina or activated carbon, as demonstrated in the case of ferrocene adsorbed on activated carbon 13,14 and triphenylphosphine oxide adsorbed on alumina.15

^a Department of Chemistry, Texas A&M University, College Station, Texas 77842-3012, USA. E-mail: bluemel@tamu.edu

^b Department of Chemistry, Colorado School of Mines, Golden, Colorado, USA. E-mail: yuanyang@mines.edu

 $[\]dagger$ Electronic supplementary information (ESI) available: Additional ^{31}P and ^{2}H solid-state and solution NMR spectra, surface coverages, linewidths, contact time characteristics and T1 relaxation times. See DOI: https://doi.org/10.1039/ d3nj03016d

We and others have previously shown that diverse species with high melting points can be adsorbed on solid supports in the absence of solvents. For example, solid metallocenes, 7-10 phosphine oxides, 11,12,15 and polycyclic aromatic hydrocarbons (PAH)¹⁶ including their chromium tricarbonyl complexes,¹⁷ can be adsorbed on a variety of surfaces by grinding the dry components with a mortar and pestle or just bringing the solid components into contact.^{8,10} The nucleus ³¹P is ideal to probe the dynamics and structures of surface-bound species containing phosphorus^{11,12,15,18} by solid-state NMR spectroscopy. 19-24

Phosphines and their adsorption are important, for example, in the field of nanoparticle catalysis, where phosphine capping ligands can be used to tune properties such as the nanoparticle size.²⁵ For adsorption on support surfaces phosphines like PH₃²⁶⁻²⁸ and allyldiphenylphosphine²⁹ have been used. For probing the Brønsted-acidic sites of sulfated zirconium oxide, diverse sterically hindered tertiary phosphines, including PPh₃, have been applied.³⁰ For this strongly acidic surface it could be demonstrated that phosphonium salts of the type R₃PH⁺ are generated.30 The silica surfaces used in this contribution are much less acidic and lack the potential to protonate even the more basic alkyldiarylphosphines, as proven by dipolar dephasing methods earlier.31

Interestingly, solid phosphines with high melting points, such as PPh3 (80 °C) and PCy3 (82 °C) have rarely been considered for adsorption studies (Fig. 1).30 The interaction of phosphines with a silica surface is expected to be weaker than for phosphine oxides, 11,12,15 as no hydrogen bonds between P=O groups and surface OH groups can form. Therefore, it is interesting to probe whether weak van der Waals interactions with a neutral silica surface suffice to overcome the lattice energy of solid phosphines. Furthermore, the moiety of PPh₃ actually interacting with the surface has to be identified. It could be one of the phenyl groups or the lone pair at the phosphorus atom. Finally, gaining insight into the mobilities of the phosphine molecules on the surface and probing the impact of phosphine adsorption on metal complexes with phosphine ligands that come into contact with silica was also investigated.

In this contribution, we demonstrate that the high-melting phosphines PPh₃ (1) and PCy₃ (2) can be adsorbed on a silica surface as 1a and 2a not only from a solution, but also by dry grinding of the components in the absence of a solvent (Fig. 1). The progress of the dry adsorption is monitored by ³¹P solid-

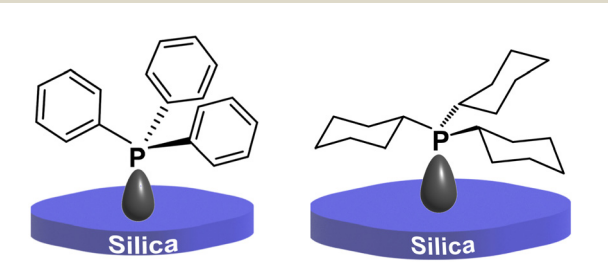


Fig. 1 Schematic display of PPh₃ (1) and PCy₃ (2) adsorbed on a silica surface as 1a and 2a.

state NMR. The averaging out of anisotropic interactions and T_1 relaxation time measurements confirm the change from polycrystalline 1 and 2 to surface-adsorbed 1a and 2a. Selectively deuterated PPh_3-d_1 ($Ph_2P(p-C_6H_4D)$, $1-d_1$), PPh_3-d_3 ($P(p-C_6H_4D)$) $C_6H_4D_3$, $1-d_3$), and PPh_3-d_5 ($Ph_2P(C_6D_5)$, $1-d_5$) allowed the additional use of ²H solid-state NMR spectroscopy to confirm the rapid motion of the adsorbed phosphine molecules across the silica surface at ambient temperature. Experiments applying the phosphine nickel complex (Ph₃P)₂Ni(CO)₂ to the surface show that silica competes for the phosphine ligands and removes them from the metal center.

Results and discussion

Polycrystalline PPh₃ (1) is a solid with a high melting point of 80 °C. Its ³¹P CP/MAS spectra, recorded at different spinning speeds, exhibit a narrow isotropic line at $\delta_{iso} = -9.4$ ppm with a halfwidth of about 70 Hz. The chemical shift is in accordance with the values reported in the literature $(-7 \text{ ppm},^{21} - 8 \text{ ppm},^{32})$ and -10 ppm^{21}) (Fig. S1, ESI†). The rotational sidebands indicate a CSA (chemical shift anisotropy) pattern^{20,21} that manifests in the wideline spectrum recorded without sample spinning. The CSA parameters are δ_{11} (7 ppm), δ_{22} (7 ppm) and δ_{33} (-43 ppm) with a span²¹ of 51 ppm. The appearance of the 4 kHz spectrum changes drastically when 1 is adsorbed on silica from a diethyl ether solution to form 1a (Fig. 2). After complete removal of the solvent, the CSA is reduced to the point where no rotational sidebands are visible any longer. This translates to averaging of the chemical shift anisotropy due to fast motion of the adsorbed molecules. They are reorienting fast and quasi-isotropically by spiraling movements on the surface within the pores of the silica.

In fact, the molecules of 1a, adsorbed in a sub-monolayer coverage (20 mg per g of silica, 7 molecules per 100 nm²) are so mobile on the silica surface that the residual linewidth of the ³¹P CP/MAS signal does not increase substantially when the spinning speed is lowered from 4 kHz (linewidth 420 Hz) to 2 kHz (550 Hz). Even when the sample is not spun at all, the residual linewidth of the signal remains comparatively small (920 Hz). As detailed below, the residual halfwidths are also dependent on the surface coverage. However, regarding one

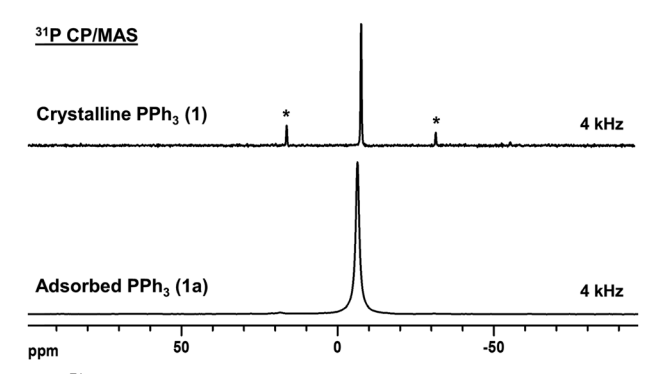


Fig. 2 ³¹P CP/MAS spectra of PPh₃ (1) (top), and PPh₃ adsorbed on silica (1a, 0.1 g on 1 g of silica) (bottom). Asterisks denote rotational sidebands.

specific surface coverage, the minimal impact of sample spinning on the halfwidth persists. For example, a monolayer coverage with 1a (206 molecules on 100 nm²) shows the same trend. The halfwidth of the ³¹P CP/MAS signal is 340 Hz at 4 kHz spinning speed and only slightly larger without sample rotation (520 Hz) (Fig. S2, ESI†). Higher rotational frequencies do not further reduce the residual linewidths in the CP/ MAS spectra.

Finally, the adsorption also manifests in a downfield shift of the ^{31}P NMR signal from -10 ppm to -6 ppm. This indicates that the free electron pair at phosphorus is interacting with either surface silanol or siloxane groups.33 Although, in contrast to triphenylphosphine oxide, no hydrogen bond in the classical sense can form, the electron withdrawing effect of the surface on the phosphorus nucleus is noticeable. The influence of the surface properties of silica on the line shape is investigated below.

In principle, the line-narrowing and CSA-reducing effects seen in the ³¹P CP/MAS spectra of **1a** could stem from partial quaternization at the phosphorus. For example, it has been demonstrated earlier that the quaternary phosphonium cations [R₃EtP]⁺ exhibit much smaller CSA values than phosphine oxides due to the higher electronic symmetry at the ³¹P nucleus.³⁴ Therefore, in order to ascertain that the molecules of 1a are translationally mobile, the ¹³C CP/MAS spectra of 1 and 1a have been recorded (Fig. 3). A sample of polycrystalline 1 gives overlapping aromatic carbon signals of the phenyl groups with the characteristically large CSA.²¹ After adsorption as 1a, the rotational sidebands vanish and the isotropic aryl signals are nearly resolved (Fig. 3). This indicates that the phenyl groups in 1 are mobile, too, since quaternization at phosphorus alone would not change the CSA of the aryl carbons.

Based on the geometry of 1, derived from the X-ray structure of PPh₃,³⁵ the phenyl groups cannot interact with the silica surface by aligning parallel to it like benzene^{36,37} without participation of the free electron pair at phosphorus. Nevertheless, some crucial interaction of the aromatic rings with the surface could occur, as the research on adsorbed PAH shows. 16,17 In order to exclude the interaction of the aromatic system with the surface as the driving force behind the adsorption, PCy3 (2) has been administered on the surface to yield 2a as described for 1a above. The ³¹P CP/MAS spectra of polycrystalline 2 show the expected large CSA with a

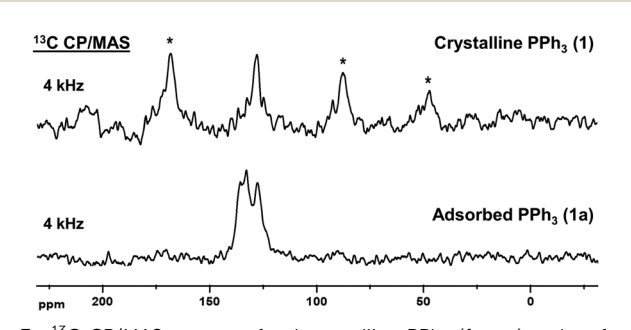
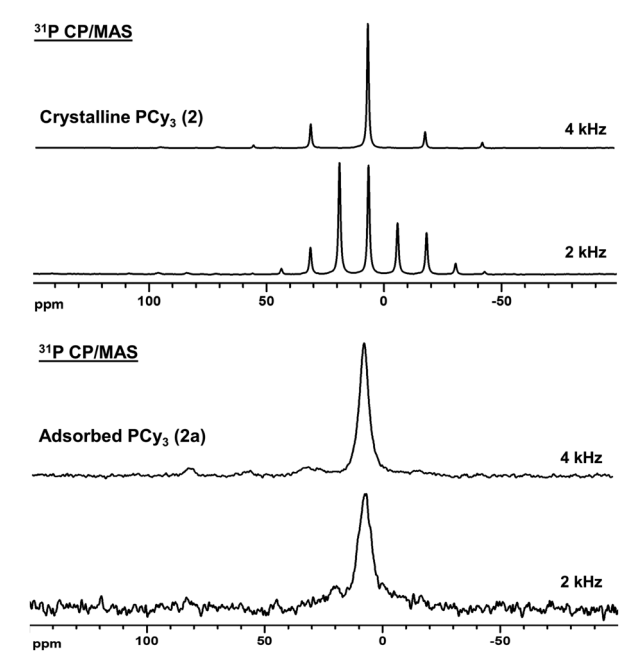


Fig. 3 ¹³C CP/MAS spectra of polycrystalline PPh₃ (1, top) and surfaceadsorbed PPh3 (1a, bottom) at 4 kHz spinning speed. The contact time for all measurements was 5 ms. Asterisks denote rotational sidebands



³¹P CP/MAS spectra of polycrystalline PCy₃ (2) (top two spectra), and PCy3 adsorbed on silica (2a) (bottom two spectra) at the indicated rotational speeds.

span²¹ of 65 ppm and the parameters δ_{11} (36 ppm), δ_{22} (13 ppm), and δ_{33} (-29 ppm), in accordance with reported values²¹ (Fig. 4) and a narrow isotropic line with a halfwidth of 110 Hz at 7 ppm. However, after adsorption, 2a yields a broadened isotropic line featuring a halfwidth of 600 Hz, but no more rotational sidebands. The drastically reduced CSA of 2a proves that the adsorption phenomenon also takes place when a solid trialkylphosphine with a high melting point is used and that it is independent of the presence of aromatic substituents at phosphorus. Therefore, it can be concluded that the adsorption is mainly driven by the lone pair at the phosphorus atom interacting with the surface.

Tertiary phosphines adsorb on the silica surface readily when applied from a solution. Interestingly, the adsorption process also takes place when the dry components are brought into contact. After manually grinding PPh3 and silica together with a mortar and pestle for an hour and then placing the mixture in a rotor, the solvent-free adsorption process can be monitored with ³¹P CP/MAS (Fig. 5). Adsorbed **1a** is already visible after one hour with a signal downfield-shifted from that of polycrystalline 1. The dry self-adsorption then progresses without further handling of the mixture over the course of 17 days.

Although the adsorption without solvent takes much longer than applying 1 from solution, it offers important insights. In general, the solvent-free adsorption presents an example illustrating that solids are not inert and react or interact with each other over time even in the absence of solvents. This is a key factor enabling mechanochemistry that typically applies higher temperatures and pressures to speed up the solvent-free reactions. Only one example of isostructural solid metallocenes forming solid solutions at ambient temperatures has been described.³⁸

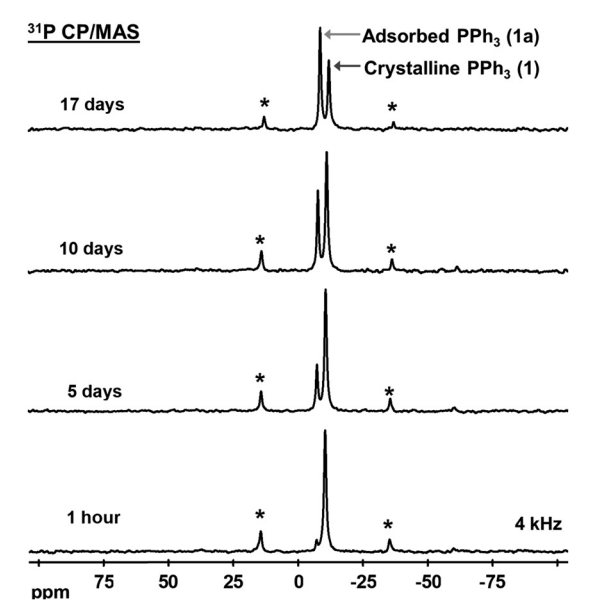


Fig. 5 ³¹P CP/MAS spectra of polycrystalline PPh₃ (1), slowly being adsorbed on silica in the absence of a solvent to form 1a, recorded at the given intervals. Asterisks denote rotational sidebands of residual 1.

Furthermore, regarding the adsorption of 1, the sequence of spectra displayed in Fig. 5 shows that the transition from polycrystalline to adsorbed molecules is abrupt. Once a monolayer of 1a on the surface is complete, excess polycrystalline 1 is left over. There is no gradual merging of the signals of 1 and 1a. This becomes even more obvious when a sample with partially adsorbed PPh3 is measured with 31P CP while spinning slowly at 2 kHz and recording the spectrum without sample rotation (Fig. 6). The polycrystalline component 1 results in the characteristic CSA pattern, while the narrow signal of 1a resides on top of it. The nicely separated signals of adsorbed and polycrystalline material allow for the determination of the maximal surface coverage once the ratio of 1 to 1a remains constant. For the silica used for this experiment the maximal monolayer surface coverage amounts to 3.076 g of 1a per 1 g of silica,

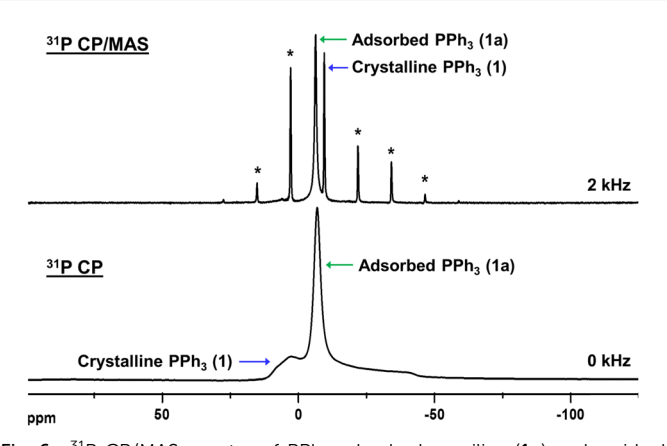


Fig. 6 31P CP/MAS spectra of PPh3 adsorbed on silica (1a) and residual polycrystalline 1 after dry-grinding and aging for 17 days. Asterisks denote rotational sidebands of residual 1.

corresponding to about 206 molecules per 100 nm² of surface area. Importantly, the maximal monolayer surface coverage is the same when 1 is adsorbed by applying a solution and subsequently removing the solvent in vacuo.

As an additional proof that polycrystalline 1 assumes a different physical state when adsorbed on the silica surface, the 31 P T_1 relaxation times of 1 and 1a, obtained by inversion recovery techniques, 19,38 were compared. While the T_1 time of polycrystalline 1 is about 1000 s,³² it is merely 0.59 s when 0.1 g of the phosphine is adsorbed on 1 g of silica (Fig. S3, S4 and Table S1, ESI†). The more than three orders of magnitude smaller value for 1a indicates the much higher mobility of the PPh₃ molecules on the surface. The T_1 relaxation time does not increase substantially when the surface coverage is increased fourfold. For example, 0.4 g of 1a on the surface of 1 g of silica leads to a value of 0.63 s (Fig. S4, ESI†). This means that the mobility remains high when quadrupling the surface coverage from about 34 molecules to 134 molecules of 1a per nm². This observation is corroborated by the dependence of the residual linewidths of the ³¹P CP/MAS signal of 1a on the surface coverage. The linewidth decreases with increasing surface coverage in the low coverage region (Fig. S5, ESI†). An example has been discussed above. This linewidth dependence is in accordance with earlier observations on covalently bound phosphines.²

Another related indicator of mobility is the CP contact time dependence. As expected for an immobile molecule residing within a crystal lattice and containing only aryl protons, for polycrystalline PPh₃ longer contact times lead to increased signal intensities (Fig. S6, ESI†).39 On the other hand, for the mobile molecules in 1a a shorter contact time of about 3 ms results in optimal signal intensity, while longer contact times lead to deteriorated S/N ratios (Fig. S6, ESI†). The proton-rich PCy₃ follows the same trend. The ³¹P CP/MAS signal of polycrystalline 2 profits from longer contact times. In contrast, 2a requires a short contact time of 0.5 ms for optimal S/N ratios (Fig. S6, ESI†). 12,33,39

Besides the CSA, heteronuclear dipolar interactions between the protons and the 31P nucleus lead to a broadening of its signal. In the CP/MAS spectra discussed above, the ¹H/³¹P heteronuclear dipolar interactions had been eliminated by high-power proton decoupling (Fig. 2 and Fig. S2, ESI†). When polycrystalline 1 is probed by ³¹P MAS using a single pulse program without proton decoupling, the residual linewidth of the signal (1.4 kHz) is large even at 4 kHz rotational frequency, while the CSA is still visible via the first order rotational sidebands (Fig. S7, ESI†). In contrast, even without highpower proton decoupling the resonance of 1a is rather narrow (420 Hz) and decoupling only leads to a moderate decrease of the residual linewidth to 360 Hz. This demonstrates that heteronuclear dipolar interactions are efficiently eliminated already by the mobility of the molecules of 1a on the surface. This becomes even more obvious when considering the wideline ³¹P spectra of polycrystalline 1 and adsorbed 1a (Fig. S8, ESI†). Without rotation and proton decoupling the signal of 1 is broad and unstructured, spanning about 7.2 kHz. Under the same measurement conditions a narrow signal is obtained for 1a (460 Hz halfwidth). Interestingly, proton decoupling

broadens the signal to 1 kHz, most probably due to interference of the decoupling frequency with the reorientation of the molecules on the surface within the pores. This broadening effect due to decoupling has been described earlier involving the ring rotation in decamethylchromocene.⁴⁰

Quadrupolar interactions lead to large signals with characteristic patterns for quadrupolar nuclei in the solid state. These patterns can be used for analytical purposes. For example, the Pake pattern of deuterium nuclei has been used widely for probing mobile species and moieties in the solid state. 13,22,41,42 Therefore, we synthesized three deuterated versions of 1, PPh₃- d_1 (Ph₂P(p-C₆H₄D), 1- d_1), PPh₃ d_3 (P(p-C₆H₄D)₃, 1-d₃), and PPh₃-d₅ (Ph₂P(C₆D₅), 1-d₅).

All ²H CP/MAS spectra of the polycrystalline deuterated phosphines show Pake patterns (Fig. 7 and Fig. S9, ESI†) with the quadrupolar coupling constants Q_{CC} 160 kHz (1- d_1) and 149 kHz (1- d_3 , 1- d_5). However, once adsorbed on silica the large quadrupolar interactions are averaged out due to the translational mobility of the molecules of $1a-d_1$, $1a-d_3$, and $1a-d_5$ on the curved surface and only the relatively narrow isotropic lines remain. Comparing the linewidths (1.5, 6.4, and 5.0 kHz) and appearances of the signals with calculated lineshapes⁴¹ shows that the maximal reorientation time corresponds to about 0.3 µs. It is noteworthy that the adsorbed phosphines do not show signals when measured with cross polarization due to their mobility.⁴³

Next, we performed preliminary studies about how the nature of the silica surface^{6,43} and its pore size influence the mobility of 1a. For the latter, the same amount of 1 was adsorbed on silica batches with average pore diameters of 40 and 100 Å. Both the chemical shifts (-6 ppm) and linewidths (230 and 200 Hz) of the ³¹P CP/MAS signals were in the same range, indicating that the pore size does not have a major impact on the mobility of the molecules of 1a on the surface (Fig. S10 and Table S2, ESI†). For probing whether the number of silanol groups on the surface makes a difference, the same amount of 1 was added to batches of silica rigorously dried in vacuo at 600 °C and "wet" silica that had been dried at ambient temperature to just remove the adsorbed water. ^{6,43} The ³¹P CP/ MAS spectra again do not show any difference (Fig. S11, ESI†). The chemical shifts and linewidths are identical (-6 ppm,230 Hz). Therefore, it can be concluded that the polarity of the surface does not play a crucial role and that the driving

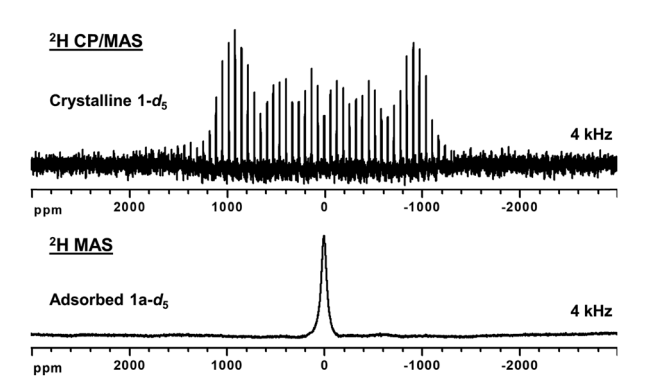


Fig. 7 ²H CP/MAS spectrum of polycrystalline **1-d₅** (top) and MAS spectrum of surface-adsorbed 1a-d₅ (bottom) at 4 kHz spinning speed.

force of the adsorption is van der Waals interactions rather than specific interactions with surface silanol groups.

Finally, Me₃Si-modified silica, generated by reacting silica with neat Me₃SiOEt, 43 has been applied to probe whether rendering the surface hydrophobic and implementing mechanical obstacles for the mobile molecules of 1a would make a difference. As the ³¹P CP/MAS spectrum shows, the adsorption takes place and the PPh₃ molecules are highly mobile across this modified surface as well (Fig. S12, ESI†). The signal halfwidth amounts to 200 Hz and is within the typical range, as is the chemical shift with -6 ppm. This result is another indicator that hydrogen bonding to silanol groups does not play a major role in the adsorption of 1 on silica. Furthermore, the Me₃Si groups do not present obstacles that would slow down the adsorbed molecules of 1a.

The adsorption of phosphines on silica surfaces is phenomenologically important. It also has implications for phosphines coordinated in metal complexes. In case the phosphines serve as linkers for immobilized catalysts, 3-5 their preferential adsorption on the numerous surface sites might lead to detachment from the metal center and leaching of the catalyst⁵ or nanoparticle formation.3 To preliminarily investigate this issue, (Ph3P)2Ni(CO)2 (3) was applied to a silica surface from a solution of the complex in THF. After removal of the solvent, the material was heated to 50 $^{\circ}\mathrm{C}$ in the dry state for three hours. The 31P MAS spectrum of the sample shows that a substantial amount of adsorbed PPh₃ (1a) is found on the surface besides 3 (Fig. S13, ESI†). It is noteworthy that the phosphine ligand becomes detached from the catalyst 3 in the absence of any substrate that could be an alternative reason for the dissociation of the phosphine ligand. This observation is in accordance with earlier results.5 When performing the catalytic cyclotrimerization of phenylacetylene with an immobilized bisphosphine dicarbonylnickel complex, uncoordinated immobilized phosphine was found. This had been interpreted as substrateinduced leaching of the catalyst. However, the results presented here show that this leaching is not necessarily due to the competition of the substrate with the phosphine for a coordination site at the nickel center. The silica surface and adsorption of the phosphines can be the culprit. Furthermore, it should be mentioned that the temperature of 50 °C is moderate regarding the temperatures applied for real-life catalytic reactions. When (Ph₃P)₂Ni(CO)₂ (3) is heated to 50 °C together with silica in THF, only the signal of 1a is visible in the ³¹P MAS spectrum after removal of the solvent (Fig. S13, ESI†). Therefore, it can be concluded that the silica surface efficiently removes the phosphine ligands from the nickel center, with the adsorption being the driving force. In contrast, 3 can be heated at 50 °C in the absence of silica in THF, a solvent with high coordinating potential, over three hours without any sign of decomposition (Fig. S13, ESI†).

Conclusion

In this contribution we could, for the first time, demonstrate that solid PPh3 and PCy3 self-adsorb on silica surfaces in the absence of a solvent. 31P solid-state NMR spectroscopy was applied as a powerful multipronged technique to describe the adsorption process and behavior of the adsorbed species. The

increased mobility of the adsorbed PPh3 molecules across the surface within the pores of silica manifests in shorter T_1 relaxation times, different contact time characteristics, and reduced anisotropic interactions visible in the solid-state NMR spectra. Importantly, the transition between a monolayer occupancy on the surface and leftover polycrystalline materials is abrupt. Therefore, the formation of multiple layers on the surface can be excluded. The properties of the surface play a subordinate role in the adsorption process. Rigorously dried silica surfaces, exhibiting fewer silanol groups, lead to similar ³¹P CP/MAS chemical shifts and linewidths as "wet" silica surfaces with a high number of silanol groups. Even Me₃Simodified silica does not change the adsorption characteristics of the phosphines. The mobilities of PPh3 molecules adsorbed on diverse silica surfaces could be further quantified by ²H solid-state NMR measurements of the selectively deuterated versions PPh_3-d_1 , PPh_3-d_3 , and PPh_3-d_5 . Finally, it could be demonstrated by stirring solutions of the complex (Ph₃P)₂Ni(CO)₂ with silica that the silica surface competes with the metal center for the phosphine ligands. Thus, the adsorption of phosphines on the silica surface plays a hitherto unrecognized role when immobilizing homogeneous catalysts on silica surfaces with phosphine linkers. The stripping of the complexes of their phosphine ligands might also open a pathway to generating single atom catalysts (SACs) in the future.⁴⁴

Experimental section

General aspects and silica

All chemicals were purified by recrystallization prior to use. Solvents were distilled over Na and kept in Schlenk flasks under a purified nitrogen atmosphere. All procedures and syntheses were performed at a Schlenk line under inert atmosphere or in a glove-box unless mentioned otherwise. The silica gel was purchased from Merck with particle sizes of 0.2 to 0.063 mm, a specific surface area of 750 m² g⁻¹ and average pore size of 40 Å and, where mentioned, 100 Å (400 m² g⁻¹). The silica was dried by oil pump vacuum at 600 °C for 6 days and stored under a nitrogen atmosphere. "Wet" silica was dried in vacuo at RT until no more water accumulated in a liquid nitrogen trap. Silica modified with Me₃Si groups was prepared by suspending 150 g of RT-dried silica in 390 ml of distilled Me₃SiOEt. The mixture was stirred at RT for 3 days, then the excess of Me₃SiOEt was decanted and the modified silica was dried in vacuo at RT until no more liquids appeared in a cooling trap.

NMR measurements

The ²H and ³¹P MAS and static NMR experiments were performed using a Bruker Avance 400 solid-state NMR spectrometer (Larmor frequencies 400 MHz for ¹H nuclei, 46.07 MHz for ²H, 100.58 MHz for ¹³C, and 161.49 MHz for ³¹P) equipped with a two-channel 4 mm MAS NMR probe head. Glycine and adamantane have been used as external references for ¹³C measurements and (NH₄)H₂PO₄ for ³¹P spectra. The standard single-pulse and cross-polarization sequences were applied for ³¹P and ²H nuclei, as described in the Results and discussion section. The relaxation delays were 6 s for ¹³C, 10 s for ³¹P, and 60 s for ²H solid-state NMR measurements. Typically, fewer than 1000 scans were sufficient for obtaining spectra of high quality, and no linebroadening had to be applied for processing.

The 31 P T_1 times were measured at a rotational frequency of 10 kHz using inversion–recovery (180° – τ – 90°) experiments with well-calibrated RF-pulses, τ variations between 0.0001 and 8 s, and with a relaxation (recycle) delay of 10 s corresponding to complete relaxation of the nuclei after each pulse cycle. The experimental inversion-recovery curves (signal intensity versus τ time) have been treated with a standard nonlinear fitting computer program (LabPlot) based on the Levenberg-Marquardt algorithm.

The ³¹P CSA parameters for PPh₃ and PCy₃ were obtained from the wideline spectra that were calculated based on the MAS spectra recorded at 2.5 kHz rotational speed using dmfit software. The asymmetry parameters η for PPh₃ and PCy₃ were 0.00 and 0.65, respectively. The precision for the CSA values was ± 1 ppm and for signal halfwidths ± 10 Hz.

Adsorption from solution

When the adsorption of phosphines on silica was carried out using a solution, the desired amount of phosphine, in the mg range as specified in the ESI,† was added to ca. 30 ml of pentane or ether, which had been distilled from sodium/benzophenone and kept under nitrogen. This solution was then added to a 5.0 g portion of dried silica under a nitrogen atmosphere and stirred for 10 h. The pentane was then removed in vacuo. The nonvolatile phosphines remained on the surface.

Dry adsorption

The solid components 1 or 2 were ground together with silica with the indicated amounts manually for 1 h under an inert gas atmosphere. Subsequent monitoring is described in the Results and discussion section.

Surface coverages of adsorbed species

The table summarizes the amounts of adsorbed species per 1 g of rigorously dried silica and the corresponding number of adsorbed molecules on 100 nm² of silica surface. The surface coverages of 1a were varied between 6.7 and 207 molecules per 100 nm² of silica surface (Fig. S5, ESI†), as discussed in the Results section. A typical value for 1a is given here.

Adsorbed	g per 1 g of silica	Molecules on 100 nm ²
1a	0.613	206
$1a-d_1$	0.572	192
1a- d_3	0.362	120
1a- d_5	0.345	114
2a	0.101	32

Syntheses of deuterated phosphines

The selectively deuterated phosphines 1-d₁, 45 1-d₃, 45-48 and 1 d_5^{49} have been mentioned in classical publications, but detailed

synthesis procedures were missing or based on the slow Grignard reactions starting from p-deuterohalobenzenes, giving low yields. Only fragmentary analytical data could be reported at that time. Therefore, new syntheses, based on the use of ⁿBuLi and starting from the inexpensive, commercially available pdibromobenzene, 50 and full characterization are provided here and the ²H NMR spectra are displayed in Fig. S14 (ESI[†]).

Synthesis of diphenyl(p-bromophenyl)phosphine (1-Br₁)

A 1.6 M solution of ⁿBuLi in hexanes (13.75 ml, 22.0 mmol) was added dropwise to a stirred solution of 1,4-dibromobenzene (5.110 g, 21.66 mmol) in 50 ml of freshly distilled diethyl ether at -78 °C under a nitrogen atmosphere. The solution was slowly warmed up to room temperature and stirred for another 2 h. Then the transparent solution was cooled to -78 °C and chlorodiphenylphosphine (3.95 ml, 22.0 mmol) was added dropwise. The reaction mixture was stirred at room temperature over night and then filtered to remove LiCl. The solvent was removed in vacuo. The final product was recrystallized from acetone at -40 °C to yield 6.977 g (20.45 mmol, 94.4%) of **1-Br₁** as a slightly yellow polycrystalline powder.

¹H NMR (acetone-d₆, 300.13 MHz) $\delta = 7.56$ (dd, ${}^{3}J_{H-H} =$ 8.3 Hz, ${}^{4}J_{P-H}$ = 0.9 Hz, 2H, P(C₆H₄Br), PCCCH), 7.41–7.38 (m, 6H, PPh₂, H_{m/p}), 7.32–7.27 (m, 4H, PPh₂, H_o), 7.20 (dd, ${}^{3}J_{H-H}$ = 8.3 Hz, $^{3}J_{P-H} = 6.8 \text{ Hz}, 2H, P(C_{6}H_{4}Br), PCCH).$ ^{13}C NMR (acetone-d₆, 75.47 MHz) $\delta = 137.87$ (d, ${}^{1}J_{P-C} = 13.5$ Hz, $P(C_{6}H_{4}Br)$, PC), 136.01 $(d, {}^{2}J_{P-C} = 20.2 \text{ Hz}, P(C_{6}H_{4}Br), PCC), 132.43 (d, {}^{3}J_{P-C} = 6.8 \text{ Hz},$ $P(C_6H_4Br)$, PCCC), 123.69 (s, CBr), 137.44 (d, ${}^{1}J_{P-C} = 11.42$ Hz, PPh₂, C_i), 134.31 (d, ${}^{2}J_{P-C}$ = 19.9 Hz, PPh₂, C_o), 129.50 (d, ${}^{3}J_{P-C}$ = 7.0 Hz, PPh₂, C_m), 129.85 (s, PPh₂, C_p). ³¹P NMR (acetone-d₆, 121.49 MHz) $\delta = -6.21$ (s). MS (HR/EI⁺) M⁺ 339.9997 (100%, calcd 340.0016, 100%), 341.9988 (97.0%, calcd 341.9996, 97.3%).

Synthesis of diphenyl(p-deuterophenyl)phosphine (1- d_1)

The Br/Li exchange was performed by adding 0.92 ml of a 1.6 M solution of ⁿBuLi in hexane (1.50 mmol) dropwise to a stirred solution of 1-Br₁ in ether at -78 °C. The solution was slowly warmed up to RT and stirred for another 2 h. The clear solution was quenched with 10 ml of D₂O and subsequently extracted with two 20 ml portions of ether. The organic phases were collected, dried over MgSO₄, and concentrated to give a colorless solid. Further purification by recrystallization from acetone at -40 °C yielded 0.340 g (1.29 mmol, 88.4%) of 1- d_1 as a colorless polycrystalline powder. M. p. 82–83 °C.

¹H NMR (acetone-d₆, 500.13 MHz) δ = 7.38–7.36 (m, 8H, DCCH, PPh₂, H_m, H_p), 7.30–7.29 (m, 6H, DCCCH, PPh₂, H_o). 13 C NMR (acetone-d₆, 125.76 MHz) δ = 138.19 (d, ${}^{1}J_{P-C}$ = 11.9 Hz, C_i), 134.37 (d, ${}^{2}J_{P-C}$ = 19.7 Hz, PPh₂, C_o), 129.32 (d, ${}^{3}J_{P-C}$ = 6.9 Hz, DCC), 129.42 (d, ${}^{3}J_{P-C} = 7.1 \text{ Hz}$, PPh₂, C_m), 129.67 (s, PPh₂, C_p). 31 P NMR (acetone-d₆, 202.45 MHz) $\delta = -5.93$ (s). 2 H NMR (acetone-d₆, 46.07 MHz) $\delta = 7.98$ (s). MS (HR/EI⁺) M⁺ 263.1001 (100%, calcd 263.0973, 100%).

Synthesis of tri(p-bromophenyl)phosphine (1-Br₃)

A solution of 1,4-dibromobenzene (4.509 g, 19.11 mmol) in 50 ml of ether was cooled to -78 °C. Then 11.95 ml of a 1.6 M solution of ⁿBuLi in hexane (19.11 mmol) was added in a dropwise manner. The reaction mixture was allowed to warm up to RT slowly and stirred for 2 more hours. The clear solution was again cooled to -78 °C and PCl₃ (0.874 g, 6.38 mmol) was added dropwise. The reaction mixture was stirred at RT over night and then filtered to remove LiCl. The solvent was completely removed in vacuo and the product recrystallized from acetone. A slightly yellow-green polycrystalline powder of the product 1-Br₃ was obtained (8.532 g, 17.10 mmol, yield 89.5%).

¹H NMR (acetone-d₆, 300.13 MHz) $\delta = 7.61$ (dd, ${}^{3}J_{H-H} =$ 8.3 Hz, ${}^{4}J_{P-H}$ = 1.2 Hz, 6 H, PCCCH), 7.23 (dd, ${}^{3}J_{H-H}$ = 8.3 Hz, $^{3}J_{P-H}$ = 9.0 Hz, 6H, PCCH). 13 C NMR (acetone-d₆, 75.47 MHz) δ = 140.91 (d, ${}^{1}J_{P-C}$ = 13.8 Hz, PC), 140.50 (d, ${}^{2}J_{P-C}$ = 20.7 Hz, PCC), 137.15 (d, ${}^{3}J_{P-C}$ = 7.1 Hz, PCCC), 128.69 (s, CBr). ${}^{31}P$ NMR (acetone-d₆, 121.49 MHz) $\delta = -8.10$ (s). MS (HR/EI⁺) M⁺ 497.7976 (100%, calcd 497.8206, 100%).

Synthesis of tri(p-deuterophenyl)phosphine $(1-d_3)$

ⁿBuLi (2.52 ml of a 1.6 M solution in hexane, 4.04 mmol) was added dropwise to a stirred solution of tri(p-bromophenyl)phosphine (0.672 g, 1.35 mmol) in 50 ml of ether at -78 °C. The reaction mixture was allowed to warm to RT slowly, and then it was stirred for 2 more hours. The clear solution was treated with 15 ml of D₂O and subsequently extracted with two 20 ml portions of ether. The organic phases were combined and dried with MgSO₄. Removal of the solvent in vacuo resulted in a white solid that was recrystallized from acetone. The product $1-d_3$ was obtained as colorless polycrystalline powder (0.305 g. 1.14 mmol, 84.5% yield). M. p. 81-82 °C.

¹H NMR (acetone-d₆, 500.13 MHz) δ = 7.37 (d, ${}^{3}J_{H-H}$ = 7.8 Hz, 6H, PCCCH), 7.29 (dd, ${}^{3}J_{H-H} = 7.8 \text{ Hz}$, ${}^{3}J_{P-H} = 8.0 \text{ Hz}$, 6H, PCCH). 13 C NMR (acetone-d₆, 125.76 MHz) δ = 138.19 (d, $^{1}J_{P-C}$ = 11.6 Hz, PC), 134.37 (d, ${}^{2}J_{P-C}$ = 19.8 Hz, PCC), 129.34 (d, ${}^{3}J_{P-C}$ = 6.9 Hz, PCCC). ³¹P NMR (acetone-d₆, 202.45 MHz) $\delta = -5.86$ (s). ²H NMR (acetone-d₆, 46.07 MHz) δ = 7.98 (s). MS (HR/EI⁺) M⁺ 265.0664 (100%, calcd 265.1097, 100%).

Synthesis of diphenyl(pentadeuterophenyl)phosphine $(1-d_5)$

A solution of bromobenzene- d_5 (1.50 ml, 14.25 mmol) in 50 ml of ether was cooled to -78 °C. Under stirring 8.9 ml of a 1.6 M solution of ⁿBuLi in hexane (14.25 mmol) was added in a dropwise manner. The solution was allowed to warm up slowly to RT and then stirred for another 2 h. The clear solution was cooled to −78 °C and ClPPh₂ (2.56 ml, 14.25 mmol) was added dropwise. The reaction mixture was stirred at RT over night and then filtered to remove LiCl. The solvent was removed in vacuo and the product $1-d_5$ recrystallized from acetone, which yielded 3.055 g (11.42 mmol, 80.1%) of a colorless polycrystalline powder. M. p. 83-84 °C.

¹H NMR (acetone-d₆, 500.13 MHz) δ = 7.39–7.37 (m, 6H, H_m/ H_p), 7.30–7.27 (m, 4H, H_o). ¹³C NMR (acetone- d_6 , 125.76 MHz). $\delta = 138.22$ (d, ${}^{1}J_{P-C} = 11.6$ Hz, C_{i}), 134.38 (d, ${}^{2}J_{P-C} = 19.7$ Hz, C_o), 129.45 (d, ${}^3J_{P-C}$ = 6.8 Hz, C_m), 129.68 (s, C_p). ${}^{31}P$ NMR (acetone-d₆, 202.45 MHz) $\delta = -6.17$ (s). ²H NMR (acetone-d₆, 46.07 MHz) $\delta = 7.98$ (s, ${}^{2}H_{m/p}$), 7.89 (s, ${}^{2}H_{o}$). MS (HR/EI⁺) M⁺ 267.1054 (100%, calcd 267.1220, 100%).

Heating (Ph₃P)₂Ni(CO)₂ (3) in solvent

(Ph₃P)₂Ni(CO)₂ (3) (52.3 mg, 0.0818 mmol) was dissolved in 10 ml of THF. The solution was heated for 3 h at 50 $^{\circ}\text{C}$ and after cooling was measured by ³¹P NMR. The spectrum showed only the signal of 3 at 35 ppm.

Heating 3 in THF in the presence of silica

(Ph₃P)₂Ni(CO)₂ (3) (12 mg, 0.018 mmol) was mixed with 1.3 g of silica. After adding 10 ml of THF the mixture was stirred at 50 $^{\circ}$ C for 3 h. Then the solvent was removed in vacuo and the resulting material was measured with ³¹P MAS. Only the signal of adsorbed PPh₃ (1a) was visible.

Dry heating of 3 on silica

Silica (1.1 g) was added to a solution of (Ph₃P)₂Ni(CO)₂ (3) (52.3 mg, 0.0818 mmol) in 10 ml of THF. The mixture was stirred for 20 min before the solvent was removed in vacuo. Then the dry material was stirred at 50 °C for 3 h and after cooling its 31P MAS spectrum was recorded. It showed the signals of residual complex 3 (32 ppm) and adsorbed PPh₃ (−6 ppm) (Fig. S13, ESI†).

Author contributions

The manuscript was written through contributions of all authors. The project management and design was led by J. B. and Y. Y. The syntheses and NMR experiments were performed by J. C. H. and Y. Y. All authors have given approval to the final version of the manuscript.

Conflicts of interest

The authors declare no competing financial interests.

Acknowledgements

This work was supported by the National Science Foundation (CHE-1900100).

References

- 1 W. D. Callister Jr., Materials Science and Engineering: An Introduction, 7th ed, John Wiley & Sons, New York, 2006.
- 2 E. Shakeri and J. Blümel, Creating Well-Defined Monolayers of Phosphine Linkers Incorporating Ethoxysilane Groups on Silica Surfaces for Superior Immobilized Catalysts, Appl. Surf. Sci., 2023, 615, 156380.
- 3 J. Guenther, J. Reibenspies and J. Blümel, Synthesis and Charactzerization of Tridentate Phosphine Ligands Incorporating Ethoxysilane Groups and Long Alkyl Chains for Immobilizing Molecular Rhodium Catalysts, Mol. Catal., 2019, 479, 110629.
- 4 S. Reinhard, P. Soba, F. Rominger and J. Blümel, New Silica-Immobilized Nickel Catalysts for Cyclotrimerizations of Acetylenes, Adv. Synth. Catal., 2003, 345, 589-602.

5 S. Reinhard, K. D. Behringer and J. Blümel, Immobilized Nickel Catalysts for Cyclotrimerizations of Acetylenes: Enhancement of Activities, Stabilities, and Lifetimes, New J. Chem., 2003, 27, 776-778.

- 6 R. P. W. Scott, Silica Gel and Bonded Phases, John Wiley and Sons, New York, 1993.
- 7 K. J. Cluff, M. Schnellbach, C. R. Hilliard and J. Blümel, The adsorption of chromocene and ferrocene on silica: A solidstate NMR study, J. Organomet. Chem., 2013, 744, 119-124.
- 8 K. J. Cluff and J. Blümel, Adsorption of Metallocenes on Silica, Chem. - Eur. J., 2016, 22, 16562-16575.
- 9 K. J. Cluff, N. Bhuvanesh and J. Blümel, Adsorption of Ruthenium and Iron Metallocenes on Silica: A Solid-State NMR Study, Organometallics, 2014, 33, 2671-2680.
- 10 J. W. Benzie, G. E. Harmon-Welch, J. C. Hoefler, V. I. Bakhmutov and J. Blümel, Molecular Dynamics and Surface Interactions of Nickelocene Adsorbed on Silica: A Paramagnetic Solid-State NMR Study, Langmuir, 2022, 38, 7422-7432.
- 11 S. Kharel, K. J. Cluff, N. Bhuvanesh, J. A. Gladysz and J. Blümel, Structures and Dynamics of Secondary and Tertiary Alkylphosphine Oxides Adsorbed on Silica, Chem. - Asian J., 2019, 14, 2704-2711.
- 12 C. R. Hilliard, S. Kharel, K. J. Cluff, N. Bhuvanesh, J. A. Gladysz and J. Blümel, Structures and Unexpected Dynamic Properties of Phosphine Oxides Adsorbed on Silica Surfaces, Chem. - Eur. J., 2014, 20, 17292-17295.
- 13 K. J. Cluff and J. Blümel, Adsorption of ferrocene on carbon nanotubes, graphene, and activated carbon, Organometallics, 2016, 35, 3939-3948.
- 14 P. J. Hubbard, J. W. Benzie, V. I. Bakhmutov and J. Janet Blümel, Ferrocene adsorbed on silica and activated carbon surfaces: a solid-state NMR study of molecular dynamics and surface interactions, Organometallics, 2020, 39, 1080-1091.
- 15 P. J. Hubbard, J. W. Benzie, V. I. Bakhmutov and J. Blümel, Disentangling Different Modes of Mobility for Triphenylphosphine Oxide Adsorbed on alumina, J. Chem. Phys., 2020, 152, 054718.
- 16 H. Günther, S. Oepen, M. Ebener and V. Francke, Magn. Reson. Chem., 1999, 37, S142-S146.
- 17 Y. Oprunenko, I. Gloriozov, K. Lyssenko, S. Malyugina, D. Mityuk, V. Mstislavsky, H. Günther, G. von Firks and M. Ebener, Chromium tricarbonyl complexes with biphenylene as η⁶ ligand: synthesis, structure, dynamic behaviour in solid state and thermal η^6 , η^6 -haptotropic rearrangements. Experimental (NMR) and theoretical (DFT) studies, J. Organomet. Chem., 2002, 656, 27-42.
- 18 I. G. Shenderovich, For Whom a Puddle Is the Sea? Adsorption of Organic Guests on Hydrated MCM-41 Silica, Langmuir, 2020, 36, 11383-11392.
- 19 V. I. Bakhmutov, Strategies for solid-state NMR studies of materials: from diamagnetic to paramagnetic porous solids, Chem. Rev., 2011, 111, 530-562.
- 20 I. G. Shenderovich and H.-H. Limbach, Solid State NMR for Nonexperts: An Overview of Simple but General Practical Methods, Solids, 2021, 2, 139-154.

21 T. M. Duncan, A Compilation of Chemical Shift Anisotropies, Farragut Press, Chicago, IL, 1990.

- 22 K. Schmidt-Rohr and H. W. Spiess, Multidimensional Solid-State NMR and Polymers, Academic Press, London, UK, 1994.
- 23 K. K. Samudrala, W. Huynh, R. W. Dorn, A. J. Rossini and M. P. Conley, Formation of a Strong Heterogeneous Aluminum Lewis Acid on Silica, Angew. Chem., Int. Ed., 2022, 61, e202205745.
- 24 S. L. Carnahan, Y. Chen, J. F. Wishart, J. W. Lubach and A. J. Rossini, Magic angle spinning dynamic nuclear polarization solid-state NMR spectroscopy of γ -irradiated molecular organic solids, Solid State Nucl. Magn. Reson., 2022, **119**, 101785.
- 25 L. M. Rossi, J. L. Fiorio, M. A. S. Garcia and C. P. Ferraz, The Role and Fate of Capping Ligands in Colloidally Prepared Metal Nanoparticle Catalysts, Dalton Trans., 2018, 47, 5889-5915.
- 26 M. H. Weston, W. Morris, P. W. Siu, W. J. Hoover, D. Cho, R. K. Richardson and O. K. Farha, Phosphine Gas Adsorption in a Series of Metal-Organic Frameworks, *Inorg. Chem.*, 2015, 54, 8162-8164.
- 27 J. Wyrick, X. Wang, P. Namboodiri, R. V. Kashid, F. Fei, J. Fox and R. Silver, Enhanced Atomic Precision Fabrication by Adsorption of Phosphine into Engineered Dangling Bonds on H-Si Using STM and DFT, ACS Nano, 2022, 16, 19114-19123.
- 28 T. V. Pavlova, G. M. Zhidomirov and K. N. Eltsov, First-Principle Study of Phosphine Adsorption on Si(001)-2 \times 1-Cl, J. Phys. Chem. C, 2018, 122, 1741-1745.
- 29 F. Sgarbossa, A. Levarato, S. M. Carturan, G. A. Rizzi, C. Tubaro, G. Ciatto, F. Bondino, I. Píš, E. Napolitani and D. De Salvador, Phosphorus Precursors Reactivity versus Hydrogenated Ge Surface: Towards a Reliable Self-Limited Monolayer Doping, Appl. Surf. Sci., 2021, 541, 148532.
- 30 J. Rodrigues, D. B. Culver and M. P. Conley, Generation of Phosphonium Sites on Sulfated Zirconium Oxide: Relationship to Brønsted Acid Strength of Surface -OH Sites, J. Am. Chem. Soc., 2019, 141, 1484-1488.
- 31 J. Blümel, Reactions of Phosphines with Silica: A Solid-state NMR Study, Inorg. Chem., 1994, 33, 5050-5056.
- 32 R. Sharma, G. P. Holland, V. C. Solomon, H. Zimmermann, S. Schiffenhaus, S. A. Amin, D. A. Buttry and J. L. Yarger, NMR Characterization of Ligand Binding and Exchange Dynamics in Triphenylphosphine-Capped Gold Nanoparticles, J. Phys. Chem. C, 2009, 113, 16387-16393.
- 33 J. Blümel, Reactions of Ethoxysilanes with Silica: A Solid-State NMR Study, J. Am. Chem. Soc., 1995, 117, 2112-2113.
- 34 J. Sommer, Y. Yang, D. Rambow and J. Blümel, Immobilization of Phosphines on Silica: Identification of Byproducts via ³¹P CP/MAS Studies of Model Alkyl-, Aryl-, and Ethoxyphosphonium Salts, Inorg. Chem., 2004, 43, 7561-7563.
- 35 B. Ziemer, A. Rabis and H.-U. Steinberger, Triclinic Polymorphs of Triphenylphosphine and Triphenylphosphine Sulfide, Acta Crystallogr., Sect. C: Cryst. Struct. Commun., 2000, 56, e58.

- 36 E. Gedat, A. Schreiber, J. Albrecht, Th. Emmler, I. Shenderovich, G. H. Findenegg, H.-H. Limbach and G. Buntkowsky, ²H-Solid-State NMR Study of Benzene-d₆ Confined in Mesoporous Silica SBA-15, J. Phys. Chem. B, 2002, 106, 1977-1984.
- 37 J. W. Benzie, V. I. Bakhmutov and J. Blümel, Benzene Adsorbed on Activated Carbon: A Comprehensive Solid-State NMR Study of Interactions with the Pore Surface and Molecular Motions, J. Phys. Chem. C, 2020, 124, 21532-21537.
- 38 G. E. Harmon-Welch, J. C. Hoefler, M. R. Trujillo, N. Bhuvanesh, V. I. Bakhmutov and J. Blümel, Creating Solid Solutions of Metallocenes: Migration of Nickelocene into the Ferrocene Crystal Lattice in the Absence of a Solvent, J. Phys. Chem. C, 2023, 127, 3059-3066.
- 39 S. Reinhard and J. Blümel, ³¹P CP/MAS NMR of Polycrystalline and Immobilized Phosphines and Catalysts with fast Sample Spinning, Magn. Reson. Chem., 2003, 41, 406–416.
- 40 J. Blümel, W. Hiller, M. Herker and F. H. Köhler, Solid-State Paramagnetic NMR Spectroscopy of Chromocenes, Organometallics, 1996, 15, 3474-3476.
- 41 J. Xiong, H. Lock, I. S. Chuang, C. Keeler and G. E. Maciel, Environ. Sci. Technol., 1999, 33, 2224-2233.
- 42 J. C. Hoefler, A. Vu, A. J. Perez and J. Blümel, Immobilized Di(hydroperoxy)propane Adducts of Phosphine Oxides as Traceless and Recyclable Oxidizing Agents, Appl. Surf. Sci., 2023, 629, 157333.
- 43 J. Blümel, Reactions of Ethoxysilanes with Silica: A Solid-State NMR Study, J. Am. Chem. Soc., 1995, 117, 2112-2113.
- 44 K. Ding, D. A. Cullen, L. Zhang, Z. Cao, A. D. Roy, L. N. Ivanov and D. Cao, A general synthesis approach for supported bimetallic nanoparticles via surface inorganometallic chemistry, Science, 2018, 362, 560-564.
- 45 E. A. Yakovleva, E. N. Tsvetkov, D. I. Lobanov, A. I. Shatenshtein and M. I. Kabachnik, Protophilic Deuteroexchange of Certain Tertiary Arylphosphines and Their Oxides, Tetrahedron, 1969, 25, 1165-1173.
- 46 R. Benassi, M. L. Schenetti, F. Taddei, P. Vivarelli and P. Dembech, ¹H Nuclear Magnetic Resonance Study of Para-Substituted Derivatives of Triphenylphosphine, J. Chem. Soc., Perkin Trans. 2, 1974, 1338-1342.
- 47 D. K. Morita, J. K. Stille and J. R. Norton, Methyl/Phenyl Exchange between Palladium and a Phosphine Ligand. Consequences for Catalytic Coupling Reactions, J. Am. Chem. Soc., 1995, 117, 8576-8581.
- 48 R. A. Baldwin and M. T. Cheng, Arylenebis(tertiary phosphines) and -(phosphinic acids), J. Org. Chem., 1966, 32,
- 49 K. Fukuda, N. Iwasawa and J. Takaya, Ruthenium-Catalyzed Ortho C-H Borylation of Arylphosphines, Angew. Chem., Int. Ed., 2019, **58**, 2850–2853.
- 50 J. H. Baker, N. Bhuvanesh and J. Blümel, Tetraphosphines with tetra(biphenyl)silane and -stannane cores as rigid scaffold linkers for immobilized catalysts, J. Organomet. Chem., 2017, 847, 193-203.